Available online at www.sciencedirect.com
SCIENCE DIRECT®
Journal of Sound and Vibration 280 (2005) 719–738
JOURNAL OF SOUND AND VIBRATION
www.elsevier.com/locate/jsvi

A two-dimensional shear deformable beam element based on the absolute nodal coordinate formulation

K.E. Dufva*, J.T. Sopanen, A.M. Mikkola

Department of Mechanical Engineering, Lappeenranta University of Technology, Skinnarilankatu 34, P.O. Box 20, FIN-53851 Lappeenranta, Finland

Received 11 November 2003; accepted 16 December 2003
Available online 3 September 2004

Abstract

In this study, a new two-dimensional shear deformable beam element is proposed for large deformation problems. The kinematics of the beam are defined using an exact displacement field, where the rotation angles of the cross-section caused by bending and shear deformations are described separately. Cubic interpolation is used for determining the curvature of the beam due to bending, while linear interpolation polynomials are used for the shear strain. The absolute nodal coordinate formulation, in which global displacements and slopes are used as the nodal coordinates, is employed for the finite element discretization of the beam. The capability of the element to predict static deformation is studied using numerical examples. The results imply that the element is free of a phenomenon called shear-locking. The capability of the element to model highly nonlinear behaviour is established using a bending test where the cantilever is bent into a full circle using only four elements. A flexible pendulum and a spin-up manoeuvre are modelled in order to study the behaviour of the element in dynamical problems. The proposed element is also compared with an existing shear deformable beam element based on the absolute nodal coordinate formulation. Finally, the simple linearization of the beam curvature based on the assumption of small strain will be discussed.

*Corresponding author. Tel.: +358-5-621-2468; fax: +358-5-621-2499.
E-mail addresses: Kdufva@lut.fi (K.E. Dufva), Jsopanen@lut.fi (J.T. Sopanen), mikkola@lut.fi (A.M. Mikkola).

0022-460X/$ - see front matter © 2004 Elsevier Ltd. All rights reserved.
doi:10.1016/j.jsv.2003.12.044

1. Introduction

The need to model geometrical nonlinearity and highly flexible beam structures has increased in a number of modelling cases. Many authors have pointed out that these topics become more important when considering multibody systems. Existing formulations for the modelling of beam-like structures, which are subject to finite rotations, have been presented, for example, by Simo and Vu-Quoc [1,2] and Cardona and Geradin [3]. These formulations are based on the geometrically exact beam theory. In this formulation, the nodal coordinates consist of absolute translational coordinates and finite rotations. An element based on this formulation is capable of representing exact rigid body rotations and is able to capture shear deformation. The drawback associated with the geometrically exact beam theory is the interpolation of finite rotations, which is often the source of complications. It is also important to note that the use of the geometrically exact beam theory leads to a nonlinear description of inertia. This is due to the nonlinear relation of the shape function matrix and the vector of the nodal coordinates. Sharf [4] has presented a method in which the motion of each body is described in a floating reference frame with an exact displacement field for beams. This formulation is based on the Euler–Bernoulli beam theory that assumes the beam cross-section to remain perpendicular to the symmetry axis of the beam.

The aim of this work is to develop a beam element that employs exact kinematics, from the Lagrangian point of view, for a planar, shear deformable Timoshenko beam. Finite element discretization is carried out using the absolute nodal coordinate formulation [5]. This recently introduced finite element formulation is well suited for the analysis of multibody systems where flexible bodies with large rotational and translational movements are considered. Unlike the floating frame of reference formulation, the absolute nodal coordinate formulation defines the displacements and slopes at the nodes in a global inertial frame of reference. Using the appropriate element shape functions, the absolute nodal coordinate formulation leads to the exact description of rigid body dynamics [6].

Various elements based on the absolute nodal coordinate formulation have been developed for beam and plate structures [7,8]. A two-dimensional shear deformable beam element for the absolute nodal coordinate formulation has already been introduced by Omar and Shabana [9]. This element formulation uses a continuum mechanics approach for the displacement field when deriving elastic forces. In the case of beams, this kind of approach should be used with care, since different-order interpolation polynomials are used for the longitudinal and transverse directions in the displacement field. Accordingly, this can lead to inaccuracies in the elastic forces, as is pointed out in Ref. [10]. In the proposed element, a continuum mechanics approach is not directly applied in the displacement field of the finite element. Instead, the proposed element employs the exact displacement field where a continuum mechanics approach is applied. The exact displacement field consists of rotations of the cross-section due to the curvature as well as due to the shear angle of the beam. These rotations can be conveniently expressed using the slopes and displacements of the element. Moreover, in the proposed element, all the strain components are treated individually, as a result of which an accurate expression can be obtained for the elastic forces.

In a traditional shear deformable beam model, linear shape functions are often used for both the displacements and the rotations. As pointed out by Bathe [11], for instance, this can lead to spurious shear strain that causes a phenomenon called shear locking. The objective of this study is

to introduce a two-dimensional mathematical model that is capable of defining the proper curvature and shear deformation of the beam without suffering from shear locking. The aim of the paper is to show that an accurate shear deformable beam element can be obtained without the need to interpolate the rotations.

2. Exact displacement field and nonlinear strains of the beam

2.1. Kinematics of the beam

The kinematics of a deformable beam can be expressed using a multibody approach in which the displacement of an arbitrary point, P, of the beam is defined according to Fig. 1. For simplicity, the local coordinate system that is located on the symmetry axis of the beam and the global coordinate system are initially coincident. In the beam, a point P_0 is located on the symmetry axis of the beam, while point P is on the normal of the symmetry axis of the beam in the initial condition.

Vector $\mathbf{u}_0$ defines the displacement of point P_0 and can be written as follows:

$$\mathbf{u}_0 = \mathbf{r}_0 - \mathbf{x}_0, \tag{1}$$

where $\mathbf{x}_0$ is the position vector of point P_0 in the initial configuration and $\mathbf{r}_0$ is the vector that defines the symmetry axis of the beam. The global displacement of an arbitrary point, P, can be defined using the rotation matrix, $\mathbf{A}$, and position vector, $\mathbf{y}_P$, as follows:

$$\mathbf{u}_P = \mathbf{u}_0 + \mathbf{A}\mathbf{y}_P - \mathbf{y}_P, \tag{2}$$

where $\mathbf{A}$ is an orthogonal rotation matrix. In a two-dimensional case, this matrix can be written as

$$\mathbf{A} = \begin{bmatrix} \cos(\theta) & -\sin(\theta) \\ \sin(\theta) & \cos(\theta) \end{bmatrix}, \tag{3}$$

where θ is the rotation angle of the cross-section.

The Euler–Bernoulli and Timoshenko beam theories are commonly used approaches for beams. Reddy [12], among others, has presented higher-order theories that relax the assumption of

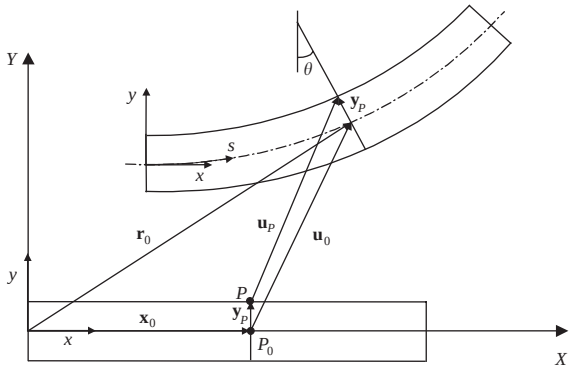

Fig. 1. The description of an arbitrary point, P, of the beam.

constant transverse shear strain throughout the thickness of the beam. This paper studies the exact displacement field for the nonlinear analysis of a shear deformable Timoshenko beam. Timoshenko beam theory relaxes the assumption of the cross-section remaining perpendicular to the symmetry axis but not that of the rigidity of the cross-section. This means that the cross-section remains plane, and thus, the shear angle is constant over the cross-section. The angle of the cross-sectional rotation in the case of a shear deformable beam is depicted in Fig. 2.

In order to capture the effect of the shear deformation in the displacement field, the overall rotation of the cross-section, θ, shown in Figs. 1 and 2, is defined as the sum of the shear angle, γ, and the angle due to the curvature of the beam, ψ, as follows:

$$\theta = \gamma + \psi. \tag{4}$$

According to Eq. (2), the exact displacement field takes the form

$$\mathbf{u}_P = \mathbf{u}_0 + \mathbf{A}_\psi \mathbf{A}_\gamma \mathbf{y}_P - \mathbf{y}_P, \tag{5}$$

where $\mathbf{A}_\gamma$ is the transformation matrix due to the shear angle, and $\mathbf{A}_\psi$ is the transformation matrix due to the curvature of the beam. The displacement field can also be written as

$$u = u_0 - y(\sin(\psi)\cos(\gamma) + \cos(\psi)\sin(\gamma)), \tag{6}$$

$$v = v_0 + y(\cos(\psi)\cos(\gamma) - \sin(\psi)\sin(\gamma)) - y. \tag{7}$$

The shear angle, γ, can be assumed to be small, $\gamma << 1$, as a result of which $\cos(\gamma)$ can be set to be equal to 1. Using this assumption, Eqs. (6) and (7) take the simplified form as follows:

$$u = u_0 - y(\sin(\psi) + \cos(\psi)\sin(\gamma)), \tag{8}$$

$$v = v_0 + y(\cos(\psi) - \sin(\psi)\sin(\gamma)) - y. \tag{9}$$

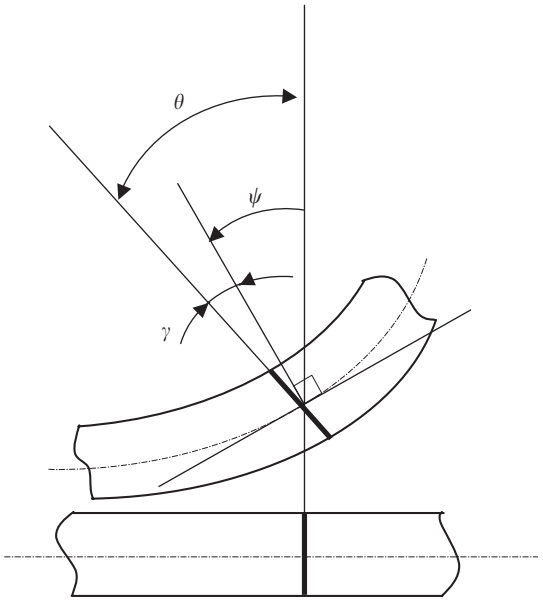

Fig. 2. The deformation angle of the cross-section of the beam.

The exact displacement field introduced in Eqs. (8) and (9) defines the displacement of an arbitrary point on the beam. This rarely used nonlinear displacement field plays a fundamental role when deriving the elastic forces and strain components in the following sections.

2.2. Strain and energy definitions

Using a continuum mechanics approach, no strains are generated in the beam during large rigid body rotation [6]. The strain tensor can be written in terms of the displacement gradient, $\bar{\mathbf{D}}$ [7]. By employing the notations from Fig. 1, the displacement gradient can be written as follows:

$$\bar{\mathbf{D}} = \frac{\partial \mathbf{u}_P}{\partial \mathbf{x}} \left[\frac{\partial \mathbf{X}}{\partial \mathbf{x}}\right]^{-1} = \bar{\mathbf{J}}\,\bar{\mathbf{J}}_0^{-1}, \tag{10}$$

where vector $\mathbf{u}_P$ is defined in Eq. (5), $\mathbf{x}$ is the vector of the local coordinates of the beam and vector $\mathbf{X}$ defines the initial configuration of the beam as $\mathbf{X} = \mathbf{S}\mathbf{e}_0$. Matrix $\bar{\mathbf{J}}_0$ is constant and is the identity matrix if the beam is not curved and the local coordinate system of the beam is initially coincident with the global coordinate system. Matrix $\bar{\mathbf{J}}$ is a displacement gradient with respect to the local coordinates x and y. The right Cauchy–Green deformation tensor can be used to define the Green–Lagrange strain tensor as follows [5]:

$$\boldsymbol{\varepsilon}_m = \tfrac{1}{2}(\bar{\mathbf{D}}^{\mathrm{T}} + \bar{\mathbf{D}} + \bar{\mathbf{D}}^{\mathrm{T}}\bar{\mathbf{D}}). \tag{11}$$

Using the linear constitutive relation, the strain energy, U, of the beam can be written as

$$U = \tfrac{1}{2}\int_V \boldsymbol{\sigma}^{\mathrm{T}}\boldsymbol{\varepsilon}\,\mathrm{d}V = \tfrac{1}{2}\int_V \boldsymbol{\varepsilon}^{\mathrm{T}}\mathbf{E}\boldsymbol{\varepsilon}\,\mathrm{d}V. \tag{12}$$

The strain vector is obtained from the strain tensor, $\boldsymbol{\varepsilon}_{\mathrm{m}}$, as follows:

$$\boldsymbol{\varepsilon} = \begin{bmatrix} \varepsilon_{xx} & \varepsilon_{yy} & 2\varepsilon_{xy} \end{bmatrix}^{\mathrm{T}}. \tag{13}$$

The constitutive relation for an isotropic material can be written as

$$\mathbf{E} = \begin{bmatrix} \lambda + 2\mu & \lambda & 0 \\ \lambda & \lambda + 2\mu & 0 \\ 0 & 0 & \mu \end{bmatrix}, \tag{14}$$

where $\lambda = Ev/[(1+v)(1-2v)]$ and $\mu = E/[2(1+v)]$.

If $\bar{\mathbf{J}}_0$ is an identity matrix, the strain components, including the second-order terms, can be expressed as

$$\varepsilon_{xx} = \frac{\partial u}{\partial x} + \frac{1}{2}\left[\left(\frac{\partial u}{\partial x}\right)^2 + \left(\frac{\partial v}{\partial x}\right)^2\right], \tag{15}$$

$$\varepsilon_{yy} = \frac{\partial v}{\partial y} + \frac{1}{2}\left[\left(\frac{\partial u}{\partial y}\right)^2 + \left(\frac{\partial v}{\partial y}\right)^2\right], \tag{16}$$

$$\varepsilon_{xy} = \frac{1}{2}\left(\frac{\partial u}{\partial y} + \frac{\partial v}{\partial x} + \frac{\partial u}{\partial x}\frac{\partial u}{\partial y} + \frac{\partial v}{\partial x}\frac{\partial v}{\partial y}\right). \tag{17}$$

3. Finite element discretization

In linear total Lagrangian formulation for a two-node C^0 beam element, the rotation of the cross-section is independent of $u_0(x)$ and $v_0(x)$. For this reason, a linear polynomial, instead of a cubic polynomial, can be used for both the displacements and the rotations, as is often the case in the Euler–Bernoulli model. When the displacement field from Eq. (5) is used, it is possible to use cubic interpolation for $v_0(x)$ and linear interpolation for the shear angle only. In the conventional mixed interpolation of the beam, an element with m nodes, the following approximations are used for the displacement field [11]:

$$v_0 \approx \sum_{i=1}^{m} S_i^{\psi} v_0^i, \quad \theta \approx \sum_{i=1}^{m} S_i^{\psi} \theta_i, \quad \gamma \approx \sum_{i=1}^{m-1} S_i^{\gamma} \gamma_i, \tag{18}$$

where S_i^{ψ} are the interpolation functions for the displacement and section rotation, correspondingly, S_i^{γ}'s are the interpolation functions for the transverse shear strain and γ_i is the shear strain at the Gauss point i [11]. Note that in Eq. (18) angles θ and γ are approximated, not their sin(-) and cos(-), as they are expressed in the exact displacement field in Eqs. (8) and (9). This is due to the assumption of small deformation within the element.

3.1. The absolute nodal coordinate formulation

In this study, a finite element procedure called the absolute nodal coordinate formulation is used to define the beam element [5]. This formulation allows for the non-incremental solution of problems involving large displacements and rotations. All nodal coordinates are defined in a global inertia coordinate system, and no infinitesimal or finite rotations are used for the rotational degrees of freedom. In the absolute nodal coordinate formulation, the element's displacement field in global coordinates can be approximated as follows [9]:

$$\mathbf{r} = \begin{bmatrix} r_1 \\ r_2 \end{bmatrix} = \begin{bmatrix} a_0 + a_1 x + a_2 y + a_3 xy + a_4 x^2 + a_5 x^3 \\ b_0 + b_1 x + b_2 y + b_3 xy + b_4 x^2 + b_5 x^3 \end{bmatrix}, \tag{19}$$

where vector $\mathbf{r}$ defines the location of an arbitrary point on the beam. Planar coordinates x and y are defined in the local coordinate system of the beam. Due to the use of the y component in the displacement field, the element is defined as a plane rather than a line. In the absolute nodal coordinate formulation, the position vector, $\mathbf{r}$, can be expressed using the shape function matrix,

S, and the vector of nodal coordinates, **e**, as

$$\mathbf{r} = \begin{bmatrix} r_1 \\ r_2 \end{bmatrix} = \mathbf{S}\mathbf{e}. \tag{20}$$

In this study, a two-node beam element, in which six nodal coordinates define each node, is used. The nodal coordinates of the element are defined using the global coordinates and slopes, as follows:

$$\mathbf{e} = \begin{bmatrix} \mathbf{e}_i^{\mathrm{T}} & \mathbf{e}_j^{\mathrm{T}} \end{bmatrix}^{\mathrm{T}} = \begin{bmatrix} \mathbf{r}_i^{\mathrm{T}} & \dfrac{\partial \mathbf{r}_i^{\mathrm{T}}}{\partial x} & \dfrac{\partial \mathbf{r}_i^{\mathrm{T}}}{\partial y} & \mathbf{r}_j^{\mathrm{T}} & \dfrac{\partial \mathbf{r}_j^{\mathrm{T}}}{\partial x} & \dfrac{\partial \mathbf{r}_j^{\mathrm{T}}}{\partial y} \end{bmatrix}^{\mathrm{T}}, \tag{21}$$

where $\mathbf{r}_i$ and $\mathbf{r}_j$ are the global position vectors of nodes i (0, 0) and j (l, 0), while l is the length of the element. The shape functions of the element must be able to describe arbitrary rigid body motion in the global coordinate system. To ensure this feature, a complete set of rigid body modes must be included in the shape functions [5]. For a two-node beam element, the shape function matrix, **S**, can be written as follows:

$$\mathbf{S} = \begin{bmatrix} S_1 & 0 & lS_2 & 0 & lS_3 & 0 & S_4 & 0 & lS_5 & 0 & lS_6 & 0 \\ 0 & S_1 & 0 & lS_2 & 0 & lS_3 & 0 & S_4 & 0 & lS_5 & 0 & lS_6 \end{bmatrix}, \tag{22}$$

where $S_1 = 1 - 3\xi^2 + 2\xi^3$, $S_2 = \xi - 2\xi^2 + \xi^3$, $S_3 = \eta - \xi\eta$, $S_4 = 3\xi^2 - 2\xi^3$, $S_5 = -\xi^2 + \xi^3$, $S_6 = \xi\eta$, $\xi = x/l$, $\eta = y/l$.

If the beam is initially coincident with the inertia coordinate system, displacement vector $\mathbf{u}_0$ can be written as

$$\mathbf{u}_0 = \mathbf{r}_0 - \begin{bmatrix} x & 0 \end{bmatrix}^{\mathrm{T}} = \begin{bmatrix} u_0 & v_0 \end{bmatrix}^{\mathrm{T}}, \tag{23}$$

where $\mathbf{r}_0$ is the position vector of point P_0 on the beam's symmetry axis according to Eq. (20) with substitution $y = 0$. In Eq. (23), x is the location of point P_0 on the symmetry axis of the beam at reference configuration (Eqs. (8) and (9)).

As pointed out by Omar and Shabana [9], vector $\partial\mathbf{r}/\partial y$ defines the cross-section of the beam. This is because any arbitrary vector in the cross-section can be described using vector $\partial\mathbf{r}/\partial y$. Vector $\partial\mathbf{r}/\partial x$, on the other hand, describes the tangent of the symmetry axis of the beam [9]. In the case of an Euler–Bernoulli beam element, these vectors remain perpendicular to each other. The curvature of the beam can be expressed independently of the cross-sectional rotation. A proper definition of the curvature becomes more important when large deformations of the beam are considered. In order to derive the proper expression for the curvature of the beam, the following relations between the centreline rotation and the displacements, as given by Hodges, are used [13]:

$$\cos(\psi) = \frac{\partial(x + u_0)}{\partial s}, \tag{24}$$

$$\sin(\psi) = \frac{\partial v_0}{\partial s}, \tag{25}$$

where x is the distance from the origin of the beam to point P at the reference condition and s is the distance along the symmetry axis of the deformed beam, as shown in Fig. 1. By differentiating

Eqs. (24) and (25) with respect to x and applying the following description for s':

$$s' = \sqrt{(1+u_0')^2 + v_0'^2}, \tag{26}$$

where $(-)'$ denotes differentiation with respect to x, Eqs. (24) and (25) can be written as

$$\cos(\psi) = \frac{1+u_0'}{\sqrt{(1+u_0')^2 + v_0'^2}}, \tag{27}$$

$$\sin(\psi) = \frac{v_0'}{\sqrt{(1+u_0')^2 + v_0'^2}}, \tag{28}$$

However, in the case of a shear deformable beam, vectors $\partial\mathbf{r}/\partial y$ and $\partial\mathbf{r}/\partial x$ may not be perpendicular due to the shear strain. In the displacement field, Eqs. (8) and (9), this is expressed using $\sin(\gamma)$ and can be derived using angle β in Fig. 3, as follows:

$$\sin(\gamma) = -\cos(\beta) = -\frac{\mathbf{r}_x^{\mathrm{T}}\mathbf{r}_y}{|\mathbf{r}_x||\mathbf{r}_y|}, \tag{29}$$

where $\mathbf{r}_\alpha = \partial\mathbf{r}/\partial\alpha, \alpha = x, y$.

In mixed interpolation, the displacements and transverse shear strains are evaluated separately. This method is traditionally used to prevent shear-locking and to create more efficient elements [11]. In the proposed element, linear shape functions can be used to approximate the shear deformation $\sin(\gamma)$ in Eq. (29). Mixed interpolation is used to achieve the linear distribution of the bending strain along the longitudinal axis. It follows that

$$\sin(\gamma) \approx \sin(\gamma)^i\left(1-\frac{x}{l}\right) + \sin(\gamma)^j\left(\frac{x}{l}\right), \tag{30}$$

where $\sin(\gamma)^i$ and $\sin(\gamma)^j$ are the components due the shear strains at the nodal points i (0, 0) and j (l, 0) of the element, respectively. Due to the constant distribution of the shear strain across the

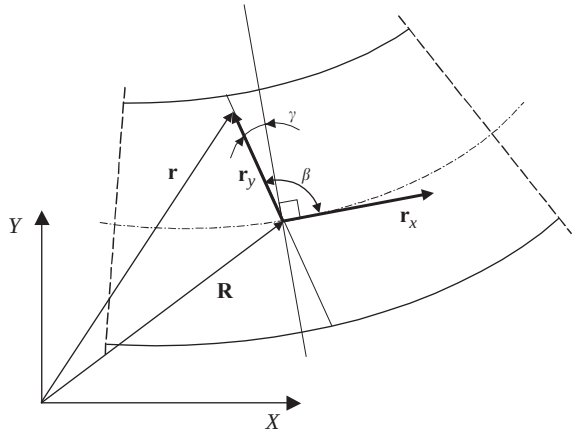

Fig. 3. The cross-section of the beam defined by vector $\mathbf{r}_y = \partial r/\partial y$.

cross-section, a cross-sectional property, k, called the shear correction factor, must be used [11]. The correction factor is a dimensionless quantity and must be evaluated separately for each shape of the cross-section. The shearing rigidity of a beam is defined as GAk.

When the vector of elastic forces is derived, the definitions of $\cos(\psi)$, $\sin(\psi)$ and $\sin(\gamma)$ are obtained from Eqs. (27), (28) and (30), respectively, and substituted into Eqs. (8) and (9). The strain components, ε_{xx} and ε_{xy}, Eqs. (15) and (17), are expressed using partial derivatives of the exact displacement field, Eqs. (8) and (9), with respect to x and y. The strain component ε_{yy} may also be obtained using partial derivatives of the displacements, Eq. (16). Due to the minor significance of this strain component in beams, the normal strain in the y-direction is often assumed to be zero, and thus, the cross-section cannot deform. However, in the proposed element, the cross-section is allowed to deform and the transverse normal strain must be defined. In this study, the simplest form of strain in the y-direction is proposed as follows:

$$\varepsilon_{yy} = \left(1 - \frac{x}{L}\right)\left|\frac{\partial \mathbf{r}}{\partial y}\right|_{x=0} + \frac{x}{L}\left|\frac{\partial \mathbf{r}}{\partial y}\right|_{x=L} - 1. \tag{31}$$

Poisson's effect will be noticed, if the strain energy of the element, Eq. (12), is calculated using the constitutive relation from Eq. (14); however, as pointed out in Ref. [10], this will lead to residual transverse normal stresses in bending and overly stiff behaviour in the element. In order to avoid this phenomenon, Poisson's effect is neglected and the height of the beam assumed to remain the same as in the initial condition unless loading is applied. The strain energy of the element can now be written as

$$U = \tfrac{1}{2}\int_V (E\varepsilon_{xx}^2 + E\varepsilon_{yy}^2 + 4kG\varepsilon_{xy}^2)\,\mathrm{d}V. \tag{32}$$

The vector of the elastic forces, $\mathbf{Q}_e$, is defined using the total strain energy, U, and the nodal vector, $\mathbf{e}$, as

$$\mathbf{Q}_e^{\mathrm{T}} = \frac{\partial U}{\partial \mathbf{e}} = \mathbf{e}^{\mathrm{T}}\mathbf{K} \tag{33}$$

In the above equation, matrix $\mathbf{K}$ represents the nonlinear stiffness matrix of the beam [5].

3.2. Generalized external forces

In the absolute coordinate formulation, external forces can be expressed using the principle of virtual work. The virtual work done by an external force, $\mathbf{F}$, applied at an arbitrary point, P, can be written as [9]

$$\delta W_e = \mathbf{F}^{\mathrm{T}}\delta\mathbf{r} = \mathbf{F}^{\mathrm{T}}\mathbf{S}\delta\mathbf{e} = \mathbf{Q}_e^{\mathrm{T}}\delta\mathbf{e}, \tag{34}$$

where $\mathbf{Q}_e$ is the generalized force vector associated with the nodal coordinates of the element. When the distributed force over the element is considered, the virtual work can be obtained by integrating Eq. (34) over the volume of the element. Also, external moments can be derived using the principle of virtual work as follows:

$$\delta W_M = M\delta\theta, \tag{35}$$

where angle θ defines the rotation of the beam section, and M is the applied external moment. The virtual change of the cross-sectional orientation can be defined using vector $\mathbf{r}_y$ as follows:

$$\delta\theta = \frac{(\partial r_2/\partial y)\,\delta(\partial r_1/\partial y) - (\partial r_1/\partial y)\,\delta(\partial r_2/\partial y)}{d}, \tag{36}$$

where $d = (\partial r_1/\partial y)^2 + (\partial r_2/\partial y)^2$ [9].

4. Equations of motion

In the absolute nodal coordinate formulation, a constant element mass matrix is defined in global coordinate system and is the same as in linear structural dynamics [5]. The elastic forces, as presented in this paper, are nonlinear functions of the nodal coordinates, as is usually the case in the absolute nodal coordinate formulation. The equation of motion of the finite element is written as [5]

$$\mathbf{M}_a\ddot{\mathbf{e}} = \mathbf{Q}, \tag{37}$$

where $\mathbf{M}_a$ is the mass matrix of the element and $\mathbf{Q}$ can be written as follows:

$$\mathbf{Q} = \mathbf{Q}_a - \mathbf{K}\mathbf{e}, \tag{38}$$

where $\mathbf{Q}_a$ is the vector of the generalized nodal forces and $\mathbf{K}$ the nonlinear stiffness matrix. The connectivity conditions of the element can be imposed as in the conventional finite element method. Due to the global definition of the coordinates, the constraint equations are often linear functions of the nodal coordinates [14].

5. Numerical examples

The numerical examples considered in this section deal with the static and dynamic behaviour of the beam. In the first static example, a cantilever beam subjected to a tip load is studied, while in the second static example the beam is bent into a full circle in order to demonstrate highly nonlinear behaviour. In these examples, the material model of the beam is considered to remain within a linear elastic range during deformation. In the first example, Young's modulus, E, is $2.07 \times 10^{11}\,\mathrm{N/m^2}$ and the shear modulus, G, is $7.9615 \times 10^{10}\,\mathrm{N/m^2}$. The correction factor, k, for the rectangular cross-section is 5/6. The cantilever structure under investigation is shown in Fig. 4.

The symmetry axis of the beam can be rotated during the deformation, and the position vector gradient in the longitudinal direction is set to be free. For this reason, all the nodal values at the clamped end of the beam, except for the slopes associated to $\partial\mathbf{r}/\partial x$, are constrained.

5.1. Linear, small-displacements tests

In the small-displacement studies, a slender beam and a stout beam with an emphasized shear effect are tested. In the case of the slender beam, the beam's width, w, is 0.1 m and its height, h, 0.1 m. In both linear cases, the tip load is set to $F = 1 \times 10^6 h^3\,\mathrm{N}$. The vertical displacement is

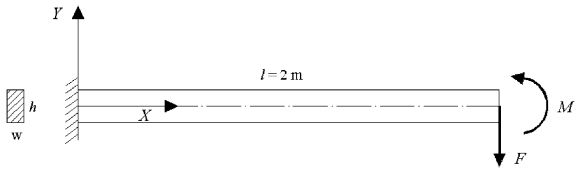

Fig. 4. The force and moment acting on the cantilever beam.

Table 1
The deformed position of the beam tip, $S_L = 1846$

Number of elements	Tip position (X, Y) (m)	
1	1.99999928036	−0.001548901
2	1.99999928035	−0.001548907
4	1.99999928035	−0.001548907
Analytical	—	−0.001548908

compared to an analytical solution obtained using the linear beam theory [15]. The results of the analyses are presented in Table 1, where the positions of the tip of the beam are shown for different numbers of elements. As can be seen from Table 1, the results match the analytical results when only one element is used. The slenderness ratio is used to describe the significance of the shear deformation in the beam under investigation. In the case of a large slenderness value ($S_L > 1000$), the Euler–Bernoulli beam theory is valid, since shear deformation does not play a significant role. The ratio is calculated as GAl^2/EI [16]. For a slender beam, the slenderness ratio (S_L) is 1846.

In Table 2, the height of the beam is increased to 1.0 m, and as a consequence the effect of shear strain becomes noticeable. In this case, the slenderness ratio is 18.5. The result using one element is practically the same as the analytical result and does not change when the number of elements is increased.

5.2. Nonlinear, large-displacement tests

Large deflections of the beam are considered for the slender beam first. The results are compared to an analytical solution by Gere and Timoshenko [15]. The analytical solution is based on the differential equation for an exact deflection curve. In this example, the applied force is obtained from the ratio Fl^2/EI that is set to 1.5. The slenderness ratio of the beam is 1.8×10^5, while the height and width of the beam are 0.01 m. The results of the analysis are shown in Table 3.

In order to study large deformations of the stout beam, the height of the beam is increased to 0.5 m, while the width of the beam is kept at 0.1 m. The applied load is set to $F = 500 \times 10^6 h^3$ N. The results for the different numbers of elements and a comparison with the same problem analysed using the ANSYS software are shown in Table 4. The ANSYS model is built using a

Table 2
The deformed position of the beam tip, $S_L = 18.5$

Number of elements	Tip position (X, Y) (m)	
1	1.99999899000221	−0.00184734183
2	1.99999899000216	−0.00184734188
4	1.99999899000216	−0.00184734188
Analytical	—	−0.00184734299

Table 3
The deformation of the beam in the nonlinear deflection analysis, $S_L = 1.8 \times 10^5$

Number of elements	Tip position and deformation angle (m and rad)		
	Tip position (X, Y)		Deformation angle
1	1.854846	−0.644362	−0.66773
2	1.800762	−0.781511	−0.63817
4	1.787239	−0.813855	−0.63775
8	1.784410	−0.821216	−0.63930
16	1.784115	−0.821955	−0.63953
Analytical	1.784	−0.822	−0.63931

Beam188 element type. It can be seen that the proposed element predicts a slightly larger deformation than does the one obtained using ANSYS.

5.3. Full circle bending test

In order to ensure the behaviour of the element in highly nonlinear cases, the moment is applied to the end of the cantilever beam. The applied moment is capable of bending the beam into a full circle. The results are compared to solutions obtained from the shear deformable element proposed by Omar and Shabana [9]. The beam is modelled using four elements. The length, l, of the cantilever structure is 1 m, cross-sectional area $1.257 \times 10^{-3}\,\mathrm{m}^2$, second moment of area $1.257 \times 10^{-7}\,\mathrm{m}^4$, Young's modulus $2.0 \times 10^8\,\mathrm{N/m}^2$. Poisson's ratio is 0. The applied external moment, M, at the end of the beam is $\lambda\pi EI/l$. The moment is given with eight substeps, and the deformation of the beam is plotted after each step. However, with the proposed element, the solution can be obtained by applying the full moment in one step only. The deformation of the proposed beam element is shown in Fig. 5. In the final configuration, the angle of the free end is 359.9°. The results obtained using the element proposed by Omar and Shabana [9] are shown in Figs. 6 and 7. When using four elements, the end tip does not reach a semicircle, which implies overly stiff element responses. The use of ten elements gives a result similar to that obtained in the previous studies for an absolute-nodal-coordinate-based beam element [17]. The error in the final angle is about 10 percent and can be decreased if more elements are used. The use of 16 elements gives a full circle.

Table 4
The nonlinear deflection for a stout beam, $S_L = 74$

Number of elements	Tip position (X, Y) (m)	
	Proposed ANCF	ANSYS
2	1.84127, −0.71394	1.86449, −0.68639
4	1.84105, −0.71450	1.85297, −0.70409
8	1.84104, −0.71452	1.85003, −0.70852
16	1.84104, −0.71452	1.84929, −0.70963

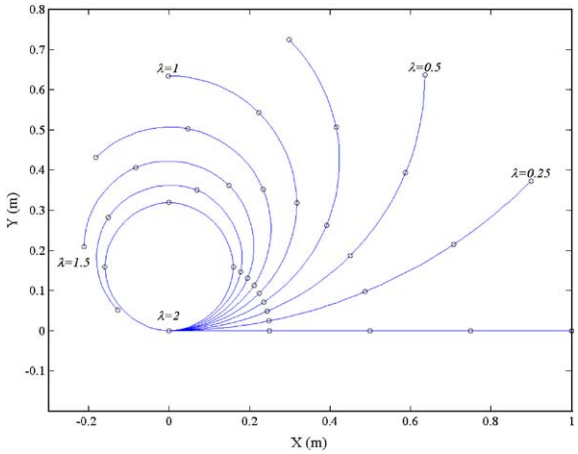

Fig. 5. The cantilever beam subjected to the tip moment using the proposed element type.

5.4. Flexible pendulum

In this section, the behaviour of the proposed element is demonstrated in a flexible dynamic simulation. The first dynamic example looks at a freefalling flexible pendulum under an evenly distributed gravity force. A beam with a rectangular cross-section is hinged with a pin joint as shown in Fig. 8. The height and width of the beam are both 0.05 m. The beam has a length of 1.2 m, second moment of area of $5.2083 \times 10^{-7}\,\mathrm{m}^4$, modulus of elasticity of $0.7 \times 10^6\,\mathrm{N/m}^2$, and mass density of $5540\,\mathrm{kg/m}^3$. Poisson's ratio is 0.3. Initially, the beam is oriented without initial velocity, as shown in Fig. 8. The gravity constant is $9.81\,\mathrm{m/s}^2$. The pendulum subjected to gravity force is a conservative system in which the total energy must remain constant during the simulation. The energy sum for the whole system is

$$\sum_{i}^{n}(T^i + U^i + V^i) = \text{const.}, \tag{39}$$

where T^i is the element kinetic energy, U^i is the strain energy, V^i is the potential energy of the element and n is the number of elements [9]. The kinetic and potential energy of the ith element are

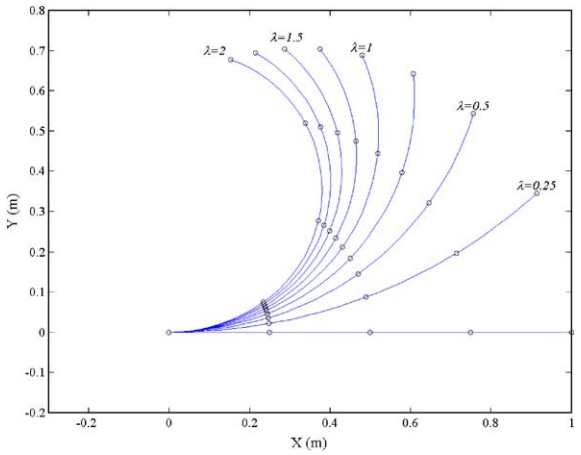

Fig. 6. The end-tip moment using comparable elements [9]; 4 elements are used.

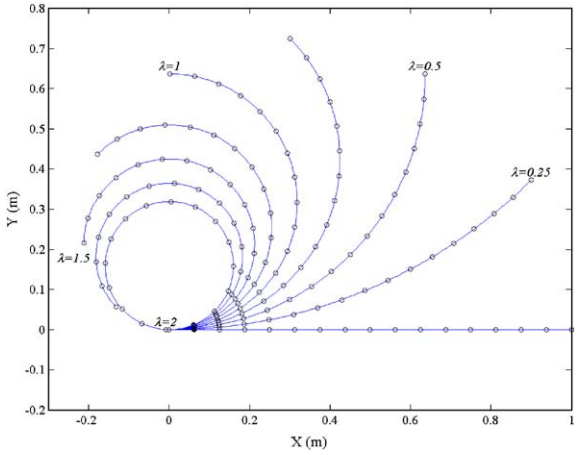

Fig. 7. The end-tip moment using comparable elements [9]; 16 elements are used.

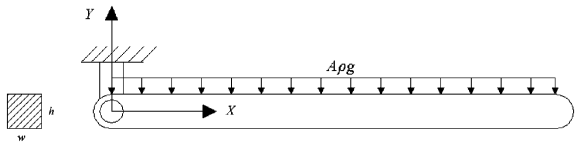

Fig. 8. A flexible pendulum in the initial state.

calculated as described in Ref. [18]. The strain energy of one element is obtained from Eq. (32). For the given initial conditions, the constant term in Eq. (39) should remain at zero. Fig. 9 shows the energy distribution between the different components as a function of time. It is worth noting that there is no energy loss during time integration. The deformations of the beam are large due to

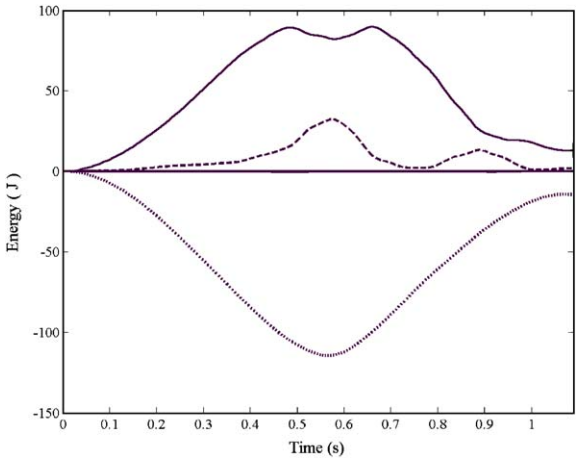

Fig. 9. The energy balance of the pendulum. —, T is the kinetic energy; - - - -, U the strain energy; … …, V the potential energy of the system. Sum of the energy is marked as —.

the flexible material and one element is not sufficient for modelling the beam. The horizontal displacement of the end tip of the beam is studied for different numbers of elements, and good convergence of the element can be obtained from Fig. 10 which shows the results obtained using 3, 6 and 12 elements. The results for 6 and 12 elements are almost the same.

The vertical displacements using the proposed element and an element obtained from Ref. [9] are depicted in Fig. 11 where the pendulum is simulated using the 6 proposed elements as well as 6 and 12 reference elements. As is to be expected from the static tests, the proposed element predicts a much larger deformation than does the element introduced by Omar and Shabana [9].

5.5. Example of a spinning beam

The so-called geometrical stiffening effect occurs when a flexible beam rapidly spins around its axis. This well-known effect caused by an axial (centrifugal) force must be coupled with a bending moment to predict the proper deformation of the beam. The element proposed in this paper is examined using the same parameters and given angular displacement θ as in the work done by Wu and Haug [19]. In this example, the angular displacement is given as

$$\theta = \begin{cases} \dfrac{\omega_s}{T_s}\left[\dfrac{1}{2}t^2 + \left(\dfrac{T_s}{2\pi}\right)^2\left(\cos\left(\dfrac{2\pi t}{T_s}\right) - 1\right)\right], & t < T_s, \\ \omega_s\left(t - \dfrac{T_s}{2}\right), & t \geq T_s. \end{cases} \tag{40}$$

The steady-state angular velocity, ω_s rad/s, is reached after T_s seconds. The beam has a length of 8 m, width of 1.986×10^{-3} m, height of 3.675×10^{-2} m, modulus of elasticity of 6.895×10^{10} N/m^2 and density of 2766.67 kg/m^3. The displacement of the end point with respect to the undeformed shadow beam obtained using an angular velocity of $\omega_s = 2$ rad/s and an acceleration time of $T_s = 15$ s is depicted in Fig. 12. The beam is defined using three elements. The exact solution for the

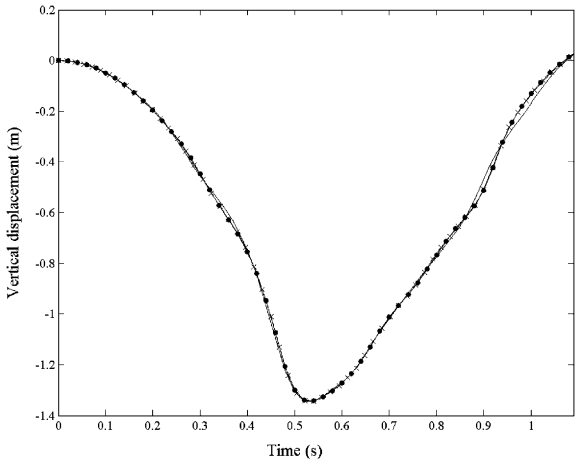

Fig. 10. The vertical displacement of the end tip of the pendulum. —, 3 elements; — × —, 6 elements; —●—, 12 elements.

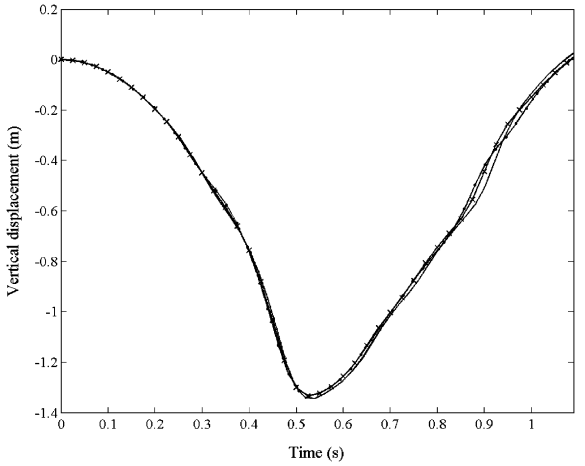

Fig. 11. A comparison between the proposed and Ref. [9] elements. —, 6 elements; —●— 6 elements [9]; — × —, 12 elements [9].

beam extension, u_x, is

$$u_x = l\left(\frac{\tan(al)}{al} - 1\right),$$
$$a = \sqrt{\frac{\rho A}{EA}}\omega_s, \tag{41}$$

where ω_s is the steady-state angular velocity [2]. According to the above equation, the extension with respect to the shadow beam is now 2.7386×10^{-5} m at the steady-state phase. The extension of the beam during the simulations (20 s) is shown in Fig. 13.

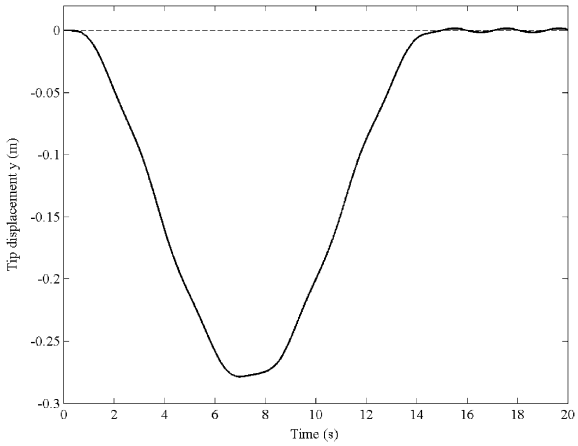

Fig. 12. The displacement of the end point, $\omega_s = 2\,\text{rad/s}$, $T_s = 15\,\text{s}$.

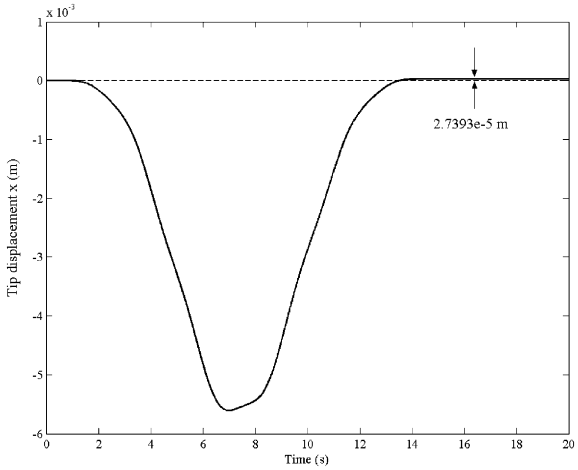

Fig. 13. The steady-state extension of the beam, 2.7393×10^{-5} m.

When the proposed beam element is used for the spinning beam problem, good agreement is achieved with the results of Refs. [2,19]. The steady-state extension of the beam is almost identical with the analytical value, and small vibrations are obtained during steady-state phase, as in the previous study with the absolute nodal coordinate formulation [20]. Based on these results, it can be said that the element is capable of capturing the geometrical stiffening effect of a spinning beam.

6. Linearization of the curvature

A simple linearization for the description of the angle due to the curvature is proposed in order to improve the computational efficiency of the element. In this simplified expression, s' can be

written as [13]

$$s' = 1 + \varepsilon, \tag{42}$$

where ε is the elongation of the neutral axis. When small strains are considered, ε is small when compared to unity. For the assumption of small strain, this simplification has no effect on the accuracy of the description of the curvature. It is important to note that this simplification does not set any restrictions on the magnitude of the rotations [13]. Eqs. (24) and (25) can be expressed in terms of the derivatives with respect to x, instead of the deformed symmetry axis s, as follows:

$$\cos(\psi) = 1 + u_0', \tag{43}$$

$$\sin(\psi) = v_0'. \tag{44}$$

This is due to the assumption that $s' = 1$.

The linearized model is tested in a full circle bending case as well as in a large-displacement test. The beam for the full circle test is the same as that used in the previous example. With the linearized model, a small overlap occurs, as can be seen in Fig. 14.

In the nonlinear large-displacement study, accurate results are also obtained when the linearized model is used. Table 5, in which the results are compared with those from Table 3,

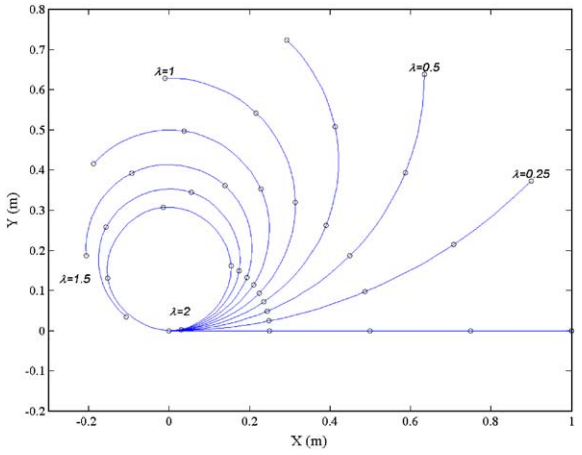

Fig. 14. The shape of the deformed beam under the load of the external moment using the linearized model.

Table 5
A comparison between the exact and linearized model under a vertical tip load

Number of elements	Tip position (X, Y) (m)	
	Exact model	Linearized model
1	1.854846, −0.644362	1.854847, −0.644358
2	1.800762, −0.781511	1.800761, −0.781508
4	1.787239, −0.813855	1.787238, −0.813851

shows that linearization does not affect the displacement of the end tip. The computation times of the linearized model are about 10 percent shorter than those of the model based on the exact description of elastic forces. When high longitudinal and transverse forces occur simultaneously, the linearized model experiences difficulties in converging to the right solution.

7. Conclusions

This paper proposes a new shear deformable planar beam element based on the absolute nodal coordinate formulation. A nonlinear continuum mechanics approach is applied to express the elastic forces of the beam. The governing equations for a two-node shear deformable beam element are developed utilizing the absolute nodal coordinate formulation, in which different-order interpolation polynomials are used for the shear angle and rotation of the cross-section. In order to achieve the linear distribution of the bending strain, the mixed interpolation technique is applied for shear strain interpolation. Due to the deformable cross-section of the beam, the y-directional strain component does not vanish and must be considered in the strain energy. This component is interpolated from the nodal values by neglecting Poisson's effect.

The static behaviour of the element is tested using numerical examples. Accurate results for small, linear deflections, as well as for larger nonlinear deflections, are obtained. The numerical results show that the response of the proposed element is accurate, also when additional deflection from shear deformation is considered. The numerical results also imply that the element does not suffer from a phenomenon called shear locking. In the example, in which a cantilever is subjected to a moment load, the element is capable of bending into a full circle using only four elements. This indicates the capability of the element to model highly nonlinear behaviour using fewer degrees-of-freedom than the previous shear deformable beam element in the absolute nodal coordinate formulation. The results for the cantilever beam are practically identical with those obtained analytically. The linearization of the components in the displacement field does not cause any noticeable inaccuracy when a vertical tip load is applied on the cantilever; however, slight crossing occurs when the beam is bent into a full circle. When the proposed element is used in dynamical simulations, computational time is saved, since fewer elements are needed due to the accuracy of the element. The element is also capable of capturing the geometrical stiffening effect in the rapidly spinning beam problem.

Acknowledgments

This study was supported by the Academy of Finland and, in part, by the National Technology Agency (Tekes).

References

[1] J.C. Simo, L. Vu-Quoc, On the dynamics of flexible beam under large overall motions—the plane case—part I, *Journal of Applied Mechanics* 53 (1986) 849–854.

[2] J.C. Simo, L. Vu-Quoc, On the dynamics of flexible beam under large overall motions—the plane case—part II, *Journal of Applied Mechanics* 53 (1986) 855–863.
[3] A. Cardona, M. Geradin, A beam finite element non-linear theory with finite rotations, *International Journal for Numerical Methods in Engineering* 26 (1988) 2403–2438.
[4] I. Sharf, Nonlinear strain measures, shape functions and beam elements for dynamic of flexible beams, *Multibody System Dynamics* 3 (1999) 189–205.
[5] A.A. Shabana, *Dynamics of Multibody Systems*, 2nd ed, Cambridge University Press, Cambridge, 1998.
[6] A.A. Shabana, Definition of the slopes and the finite element absolute nodal coordinate formulation, *Multibody System Dynamics* 1 (1997) 339–348.
[7] R.Y. Yakoub, A.A. Shabana, Three dimensional absolute nodal coordinate formulation for beam elements: implementation and application, *Journal of Mechanical Design* 123 (2001) 614–621.
[8] A.M. Mikkola, A.A. Shabana, A non-incremental finite element procedure for the analysis of large deformations of plates and shells in mechanical system applications, *Multibody System Dynamics* 9 (2003) 283–309.
[9] M.A. Omar, A.A. Shabana, A two-dimensional shear deformation beam for large rotation and deformation, *Journal of Sound and Vibration* 243 (3) (2001) 565–576.
[10] J. Sopanen, A. Mikkola, Studies on the stiffness properties of the absolute nodal coordinate formulation for three-dimensional beams, in: *Proceedings of the 2003 ASME Design Engineering Technical Conferences and Computers and Information in Engineering Conference*, DETC2003/VIB-48325, 2003.
[11] K.J. Bathe, *Finite Element Procedures*, Prentice-Hall, Englewood Cliffs, NJ, 1996.
[12] J.N. Reddy, On locking-free shear deformable beam finite elements, *Computer Methods in Applied Mechanics and Engineering* 149 (1997) 113–132.
[13] D.H. Hodges, Proper definition of curvature in nonlinear beam kinematics, *AIAA Journal* 22 (1984) 1825–1827.
[14] J.L. Escalona, H.A. Hussien, A.A. Shabana, Application of the absolute nodal co-ordinate formulation to multibody system dynamics, *Journal of Sound and Vibration* 214 (5) (1998) 833–851.
[15] J.M. Gere, S.P. Timoshenko, *Mechanics of Materials*, 2nd edition, Van Nostrand Reinhold (UK), Wokingham, UK, 1987.
[16] ANSYS User's Manual, *Theory*, 12th edition, SAS IP, Inc.©, 2001.
[17] M. Campanelli, M. Berzeri, A.A. Shabana, Performance of the incremental and non-incremental finite element formulations in flexible multibody problems, *Journal of Mechanical Design* 122 (2000) 498–507.
[18] M. Berzeri, A.A. Shabana, Development of simple models for the elastic forces in the absolute nodal co-ordinate formulation, *Journal of Sound and Vibration* 235 (4) (2000) 539–565.
[19] Shih-Chin Wu, J. Haug, Geometric non-linear substructuring for dynamic of flexible mechanical systems, *International Journal for Numerical Methods in Engineering* 26 (1988) 2211–2226.
[20] M. Berzeri, A.A. Shabana, Study of the centrifugal stiffening effect using the finite element absolute nodal coordinate formulation, *Multibody System Dynamics* 7 (2002) 357–387.